Published in final edited form as:
Exp Neurol. 2012 August ; 236(2): 298–306. doi:10.1016/j.expneurol.2012.04.013.

Isobaric tagging-based quantification by mass spectrometry of differentially regulated proteins in synaptosomes of HIV/gp120 transgenic mice: Implications for HIV-associated neurodegeneration

Sugato Banerjee[a], **Lujian Liao**[b], **Rossella Russo**[a,1], **Tomohiro Nakamura**[a], **Scott R. McKercher**[a], **Shu-ichi Okamoto**[a], **Florian Haun**[a], **Rana Nikzad**[a], **Rameez Zaidi**[a], **Emily Holland**[a], **Alexey Eroshkin**[c], **John R. Yates III**[b], and **Stuart A. Lipton**[a,*]

[a]Del E. Webb Center for Neuroscience, Aging, and Stem Cell Research, Sanford-Burnham Medical Research Institute, La Jolla, CA 92037

[b]Department of Chemical Physiology, The Scripps Research Institute, La Jolla, CA 92037

[c]Bioinformatics Shared Resource, Sanford-Burnham Medical Research Institute, La Jolla, CA 92037

Abstract

HIV/gp120 transgenic mice manifest neuropathological features similar to HIV-associated neurocognitive disorders (HAND) in humans, including astrogliosis, microglia activation, and decreased neuronal synapses. Here, proteomic screening of synaptosomes from HIV/gp120 transgenic mice was conducted to determine potential neuronal markers and drug targets associated with HAND. Synaptosomes from 13 month-old wild-type (wt) and HIV/gp120 transgenic mouse cortex were subjected to tandem mass tag (TMT) labeling and subsequent analysis using an LTQ-Orbitrap mass spectrometer in pulsed-Q dissociation (PQD) mode for tandem mass spectrometry (MS/MS). A total of 1301 proteins were identified in both wt and HIV/gp120 transgenic mice. Three of the most differentially-regulated proteins were validated by immunoblotting. To elucidate putative pathways associated with the proteomic profile, 107 proteins manifesting a ≥1.5 fold change in expression were analyzed using a bioinformatics pathway analysis tool. This analysis revealed direct or indirect involvement of the phosphotidylinositol 3-kinase (PI3K)/protein kinase B (Akt) pathway, a well-known neuronal survival pathway. Immunoblots confirmed a lower phospho (p)Akt/Akt ratio in synaptosomes from HIV/gp120 transgenic animals compared to wt, suggesting that this neuroprotective pathway was inactivated in the HIV/gp120 transgenic brain. Based on this information, we then compared immunoblots of pAkt/Akt in the forebrains of these mice as well as in human postmortem brain. We observed a significant decrease in the pAkt/Akt ratio in synaptosomes and forebrain of HIV/gp120 transgenic compared to wt mice, and a similar decrease in human forebrain from HAND

*Corresponding author: Stuart A. Lipton M.D., Ph.D., Address: 10901 North Torrey Pines Road, La Jolla, CA 92037, slipton@sanfordburnham.org, Phone: 858 795-5261, Fax: 858 795-5262.
[1]Present Address: Department of Pharmaco-Biology, Faculty of Pharmacy, University of Calabria, 87036 Cosenza, Italy

Supplementary materials related to this article can be found online at doi:xxxxxx/j.expneurol.xxxxxxxxxxx.

The authors declare that they have no competing interests.

patients compared to neurologically unimpaired HIV+ and HIV- controls. Moreover, mechanistic insight into an additional pathway for decreased Akt activity in HIV/gp120 mouse brains and human HAND brains was shown to occur via S-nitrosylation of Akt protein, a posttranslational modification known to inhibit Akt activity and contribute to neuronal cell injury and death. Thus, MS proteomic profiling in the HIV/gp120 transgenic mouse predicted dysregulation of the PI3K/Akt pathway observed in human brains with HAND, providing evidence that this mouse is a useful disease model and that the Akt pathway may provide multiple drug targets for the treatment of HIV-related dementias.

Keywords

Proteomics; gp120; HIV-1; Akt; synaptosomes; tandem mass tag labeling for Mass Spectrometry; S-nitrosylation

Introduction

Human immunodeficiency virus (HIV)-1 infection can lead to motor and cognitive impairment designated HIV-associated neurocognitive disorders (HAND) (Kaul et al., 2007; Kolson, 2002; McArthur, 2004; Meucci et al., 2000). With the advent of Highly-Active Antiretroviral Therapy (HAART) there has been a significant decline in morbidity and mortality from Acquired Immunodeficiency Syndrome (AIDS), but HIV-associated neurologic complications are increasing in prevalence (McArthur, 2004; McArthur et al., 2010). Hence, a better understanding of the neurological disease process is necessary for successful intervention. Among several rodent models of HAND, including HIV-subacute combined immunodeficiency mice (HIV/severe combined immunodeficiency [SCID] mice) (Gorantia et al., 2007; Potula et al., 2005), the HIV/gp120 envelope protein-expressing transgenic mouse has been shown to develop several neuropathological features associated with HAND, such as dendritic and synaptic damage (Garden et al., 2002; Toggas et al., 1994), and hence is useful in studying HIV neuropathogenesis.

To specifically study potential pathways involved in neuronal damage, we sought to eliminate the ~90% of brain cells that are of glial origin (Hansson and Ronnback, 2003). One effective way of enriching for neuronal proteins related to synaptic function is through isolation of synaptosomes (Cohen and Fischbach, 1977; Kennedy et al., 1983); this is particularly relevant in the case of HAND since synaptic damage is a major feature of the disease. Here we used cortical synaptosomal preparations for isobaric labeling followed by tandem mass spectrometry (MS/MS) analysis for proteomic screening of neuronal proteins.

Concerning the method of proteomic analysis, a number of techniques involving isotopic tags have been developed for the quantification of proteins and peptides (Che and Fricker, 2005; Gygi et al., 1999; Ross et al., 2004). Isotope Coded Affinity Tag (ICAT) labels react with the thiol group of cysteine residues, and, when combined with biotin-affinity tags, allow purification of the labeled peptide (Gygi et al., 1999). However, since many peptides do not contain thiol groups, ICAT labeling proved to be a relatively inefficient way of protein screening. Therefore, we chose to use isotopic labeling of primary and secondary amines and lysine side chains using isobaric tags like tandem mass tag (TMT) (Che and Fricker, 2005). Specifically, TMT6 permits simultaneous identification and relative quantification of six different extracts by labeling with six isobaric tags in the MS/MS mode. Each isobaric tagging reagent has the same precursor mass and is composed of an amine-reactive NHS-ester group, a spacer arm, and an MS/MS reporter. For each sample, a unique reporter mass results in the MS/MS spectrum (126-131 Da for TMT6). These reporter ions

are in the low mass region of the MS/MS spectrum and are used to report relative protein expression levels during peptide fragmentation (Thermo Fisher Scientific, Rockford, IL).

In this study we used TMT-based quantitative proteomic profiling followed by bioinformatics pathway analysis, which revealed dysregulation of the phosphoinositol-3 kinase (PI3K)/Akt pathway in HIV/gp120 transgenic mouse brain. Immunoblot analysis in brains of HIV/gp120 transgenic mice and humans manifesting HAND confirmed that reduced phosphoAkt (pAkt) activity strongly correlates with HIV-1 neuropathogenesis. Also, S-nitrosylated Akt was found in both HIV/gp120 transgenic mouse brains and human HAND brains, suggesting an additional mechanism for the decrease in Akt activity and consequent cell damage. These results provide evidence for the involvement of Akt in the etiology of HAND and further validating the Akt pathway as an attractive target for therapeutic intervention.

Material and Methods

Isolation of synaptosomes

Age-matched (13 month) wild-type (wt) and HIV/gp120 transgenic mice were sacrificed, and the brains were quickly removed, dissected, and then frozen with liquid nitrogen. Cortices from multiple (≥ 3) mice from the same age group were homogenized together in 0.32 M sucrose, 4 mM HEPES, and protease inhibitors. The synaptosomes were isolated using centrifugation by sucrose gradient as previously described (Carlin et al., 1980). Further purification was obtained by passing through 10 μm Millipore filters.

Tandem mass tag (TMT) labeling

To each sample of 100 μg protein we added 45 μl of 200 mM triethyl ammonium bicarbonate (TEAB) and adjusted the final volume to 100 μl with ultrapure water. Then, 5 μl of a 200 mM tris(2-carboxyethyl)phosphine (TCEP) solution was added to the mixture, and the sample was incubated at 55 °C for 1 hour × 2. Six volumes (~1 ml) of pre-chilled (-20 °C) acetone were used for overnight precipitation. The following morning, 100 μg of the acetone-precipitated protein pellets were resuspended in 100 μl of 200 mM TEAB. Trypsinization (using 2.5 μg per 100 μg protein) was carried out at 37 °C overnight. Digested peptides were tagged with the Thermo Scientific TMT6 plex Isobaric Mass Tagging Kit (wt with TMT^{126} and gp120 with TMT^{127}) according to the manufacturer's instructions. The chemically tagged samples were combined into one tube and stored at −80 °C until further use.

Protein identification by liquid chromatography (LC)-MS/MS

After the proteins were labeled with TMT, 90% formic acid was added to each sample to adjust the pH to ~2.5. Protein samples derived from either wt or HIV/gp120 transgenic mice were mixed, and 100 μg of the mixture were pressure-loaded onto a 250 μm internal diameter (I.D.) fused silica capillary column packed with 3 cm of 5 μm Partisphere strong cation exchanger (SCX, Whatman, Clifton, NJ) and 3 cm of 10 μm Jupiter reversed-phase C12 material (Phenomenex, Ventura, CA). The SCX end was fitted with immobilized Kasil 1624 (PQ Corporation, Valley forge, PA). After desalting for 1 hr, a 100 μm I.D. capillary (with a 5 μm-pulled tip that was packed with 15 cm of 4 μm Jupiter C12 material) was attached via a zero-dead-volume union, and the entire split-column was placed inline with an Eksigent nano high pressure liquid chromatography (HPLC) pump (Eksigent, Dublin, CA). Sample analysis was performed using a modified, ten-step multidimensional protein identification technology (MudPIT) described previously (Washburn et al. 2001). As peptides were eluted from the microcapillary column, they were electrosprayed directly into a hybrid LTQ-Orbitrap mass spectrometer (ThermoFinnigan, San Jose, CA) with application

of a distal 2.4 kV spray voltage. A cycle of one full-scan mass spectrum (400-1400 m/z) followed by 6 data-dependent, pulsed Q collision induced dissociation (PQD) activated MS/MS spectra was repeated continuously throughout each step of the multidimensional separation. A total of 5×10^4 ions were accumulated in the linear ion trap before PQD was performed. The PQD parameters were set as follows: 29% normalized collision energy, 0.55 active Q, and 0.4 millisecond activation time.

Processing of mass spectra and protein identification

MS/MS spectra were searched with the SEQUEST algorithm (Eng et al., 1994) against the European Bioinformatics Institute (EBI) mouse International Protein Index (IPI) database (version 3.52, release date November 21, 2008) concatenated to a decoy database in which the sequence for each entry in the original database was reversed. Static modification of lysine residues and the N-terminus of each peptide as the result of TMT reaction was set as 229.1629. The search results were assembled and filtered using the DTASelect program (Tabb et al., 2002) with a peptide false-positive rate of 1%. All peptides identified were at least 50% trypsinized, and precursor ion mass tolerance was set to 20 parts per million (ppm). Extraction of the reporter ion information was performed using Census software (Park et al., 2008). Based on peptide identification, the intensity of the same reporter ion (either 126 representing wt or 127 representing HIV/gp120 transgenic mice) from all MS/MS spectra matching a given peptide were summed to derive an intensity value for the peptide. At the protein level, all intensity values for each peptide were again summed to derive an intensity value for the protein.

Ingenuity bioinformatics pathway analysis

The list of differentially expressed proteins was submitted for pathway analysis using the Ingenuity Pathway Analysis tool (IPA, Ingenuity Inc.). A change of at least ±1.5-fold in protein abundance was considered significant (Park et al., 2008; Schrimpf et al., 2005; Witzman et al., 2005). These proteins were mapped to the corresponding protein/gene objects in the Ingenuity Pathways Knowledge Base and designated as focus genes. These focus genes were then used as the starting point for generating biological networks using the IPA software. Default parameters of network building were used with a maximum network size of 35 genes/proteins. The IPA software queried the Ingenuity Pathways Knowledge Base for interactions between focus genes and all other gene objects stored in the knowledge base, and generated a set of networks with associated statistics. The statistical likelihood score for each network was then computed according to the fit of our dataset. This score is derived from a *P*-value and indicates the likelihood of the focus genes in a network being found together due to random chance. Graphical representations of molecular relationships between genes or gene products were designated as nodes, and the biological relationship between two nodes was represented with a line. Each line was supported by literature references stored in the Ingenuity Pathways Knowledge database (www.ingenuity.com).

Immunoblot analysis

To validate differentially expressed proteins obtained by proteomic screening, Western blot analysis was conducted on isolated synaptosomes. Determination of phospho(p)Akt and Akt levels were conducted on synaptosomes from mouse cortex, cytosolic/membrane fraction of mouse forebrain, and post-mortem human cortex by Western blot analysis. Protein concentration was determined using a BCA Protein Assay (Pierce Biotechnology Inc., Rockford, IL, USA). Proteins were separated on 4-12% NU-PAGE gels (Invitrogen, Carlsbad, CA, USA) and transferred onto polyvinylidene fluoride (PVDF) membrane (Immobilon-P, Millipore). After blocking with 5% non-fat milk in Tris-buffered saline containing 0.05% Tween 20, the membranes were incubated with primary antibodies overnight at 4 °C followed by horseradish peroxidase-conjugated secondary antibody for 1

hr at RT. Protein bands were visualized with enhanced chemiluminescent detection reagents (ECL, Amersham Biosciences, GE Healthcare, Pittsburgh, PA) and exposed to X-ray film (Hyperfilm ECL, Amersham Bioscience). Autoradiographic films were scanned and densitometric analysis was performed. A Student's *t*-test was used to compare pAkt/Akt levels (densitometry) between wt and HIV/gp120 transgenic animals (synaptosome/forebrain). A one-way Analysis of Variance (ANOVA) followed by post-hoc Tukey's test was used to compare pAkt/Akt levels among HIV-, HIV+/Unimpaired and HIV+/HAND groups.

The following primary antibodies were used: rabbit polyclonal antibody against Akt, pAkt (Ser 473), pAkt (Threonine 308), Vimentin, PSD95 (Cell Signaling Technology, Beverly, MA, USA), glial fibrillary-associated protein (GFAP) (Sigma Aldrich St Louis MO), and β-arrestin (Abcam, Inc., Cambridge MA). Horseradish peroxidase-conjugated goat anti-mouse (Pierce Biotechnology, Rockford, IL, USA), Synapsin-1 (Fisher Scientific) and anti-rabbit (Biorad Hercules, CA) IgG were used as secondary antibodies.

Biotin-switch assays

To analyze S-nitrosylated protein, the biotin-switch assay was performed as described previously with modifications (Jaffrey et al., 2001). Cell lysates or brain tissue extracts were prepared in HENTS or HENC buffer (100 mM Hepes, pH 7.4, 1 mM EDTA, 0.1 mM Neocuproine, 1% Triton X-100, 0.1% SDS or 0.4% CHAPS). Approximately 300 μg of brain tissue lysate was used for each assay. Blocking buffer (2.5% SDS, 10 mM methyl methane thiosulfonate [MMTS] in HEN buffer [100 mM Hepes, pH 7.4, 1 mM EDTA, and 0.1 mM Neocuproine]) was mixed with the samples and incubated for 20 min at 50 °C with frequent vortexing to block free thiol groups. After removing excess MMTS by acetone precipitation, nitrosothiols were reduced to thiol with 20 mM ascorbate. Newly formed thiols were linked with the sulfhydryl-specific biotinylating reagent *N*-[6-(biotinamido)hexyl]-3'-(2'-pyridyldithio)propionamide (Biotin-HPDP). Unreacted Biotin-HPDP was removed by acetone precipitation and centrifugation, and the pellet was resuspended in 100 μl HENS (HEN plus 1.0% SDS). Two volumes of neutralization buffer (20 mM Hepes, pH 7.4, 100 mM NaCl, 1 mM EDTA, and 0.5% Triton X-100) were added, and the solution was cleared by centrifugation in order to pellet any debris not dissolved. Five to ten percent of the supernatant was used as the input for the control blot, and biotinylated proteins were pulled-down with Neutravidin-agarose beads (Pierce) from the remaining supernatant. Beads were washed five times, resuspended in 10 ml of NuPAGE LDS sample buffer (Invitrogen), boiled at 95 °C for 5 min, and subjected to immunoblot analysis.

Results

Isolation and proteomic screening of synaptosomes

We prepared synaptosomes as described in the Methods section from 13 month-old wt and HIV/gp120 transgenic mice, as evidenced by enrichment of synaptic markers (e.g., postsynaptic density protein 95 (PSD95) and pre-synaptic synapsin) in the synaptosomal fraction compared to crude homogenate (Fig. 1A). Synaptosomes were then subjected to TMT labeling and subsequent PQD multidimensional LC-MS/MS-based proteomic analysis performed in duplicate. The MS analysis detected a total of 1301 proteins, of which 107 proteins manifest a change ≥ 1.5 fold in HIV/gp120 transgenic mice compared to wt. Among these, 76 proteins manifested an increase and 31 proteins a decrease (Table 1). Three of the differentially-regulated proteins identified by this proteomic analysis were validated by Western blot analysis (Fig. 1B).

Ingenuity pathway analysis of differentially regulated proteins

We next examined the potential biological signaling networks underlying the differential proteomic profile with a dynamic pathway-modeling tool, Ingenuity Pathway Analysis (IPA), which is commonly used on proteomics data sets. In this standard analysis, cutoffs for protein level changes between wt and transgenic mice were made by considering that most proteins do not show any change, many-fold changes in protein levels likely represent biological significance, and at least fifty proteins must show significant fold-changes in a pathway in order to identify a pathway of potential interest. Published work and our initial analysis revealed that plotting fold-change (FCH) values showed a sharp drop in the number of proteins identified when FCH > |1.5|. The 1.5 FCH cutoff corresponds to approximately 1.25 standard deviations from the mean, and the sharply reduced number of proteins fitting this criterion is consistent with the notion that this cutoff may represent a biologically significant change. The proteins manifesting > 1.5-fold change in HIV/gp120 transgenic mice compared to wt were therefore identified to be of interest and their corresponding genes selected for IPA. The IPA module then plotted the corresponding gene networks (see Methods). The highest scoring (most statistically significant) network generated by IPA revealed involvement of PI3K/Akt pathway for the differential protein profile of HIV/gp120 mice synaptosomes compared to their age matched wt controls (Fig. 2).

Relationship of Akt and HIV-associated neurocognitive disorders (HAND)

We next examined the levels of pAkt/Akt in HIV/gp120 transgenic mouse brain and in human postmortem brains from HIV+ individuals with and without HAND vs. controls. Synaptosomes from HIV/gp120 transgenic mice manifested a significant ($P < 0.04$) decrease in the level of pAkt/Akt compared to wt controls (Fig. 3A). Additionally, we performed a similar analysis on mouse brain cytosolic lysates prepared from frontal cortex and again observed a significant ($P < 0.01$, $n = 3$) decrease in pAkt/Akt compared to age-matched littermate control mice (Fig. 3B). We then conducted similar experiments on human frontal cortex obtained relatively rapidly postmortem from normal CNS, HIV+/ neuropsychologically unimpaired, and HIV+/impaired (HAND) patients (Table 2). The diagnosis of HAND was determined by Neuropsychological testing during life, and the brains were also examined postmortem for neuropathological correlates of disease (Cherner et al., 2002; Garden et al., 2002; Moore et al., 2006; Schifitto et al., 2007). Brains from HIV-/cognitively unimpaired patients displayed a significant increase in pAkt/Akt levels compared to the HIV+/cognitively unimpaired and HAND groups, with the largest decrease in pAkt manifested in the HAND brains (Fig. 3C). A decrease in Akt enzymatic activity is known to be associated with neuronal cell injury and death; to account for the inhibition in enzyme activity, in addition to a decrease in pAkt, in HIV/gp120 mouse brains and human HAND brains we also found an increase in S-nitrosylation of Akt, which has also been shown to inhibit Akt activity (Yasukawa et al., 2005; Numajiri et al., 2011). To monitor the levels of S-nitrosylated Akt (forming SNO-Akt), we performed biotin-switch assays on brain lysates from HIV/gp120 mice and human HAND patients. Both sets of tissues revealed significant increases in SNO-Akt protein compared to controls (Fig. 4). These proteomic results are consistent with the notion that decreased Akt activity might be associated with the pathogenesis of HAND.

Discussion

In the present study, using TMT tags and multidimensional LC-MS/MS, we identified 1301 proteins in the synaptosomal compartment of the brains of HIV/gp120 transgenic and wt littermate control mice. Among these 1301 proteins, 107 showed a greater than 1.5-fold change in the HIV/gp120 transgenic mice compared to the wt controls. Confirming the validity of our techniques, we found a number of neuronal and synapse-specific proteins,

including vesicle-associated membrane protein (VAMP/synaptobrevin), syntaxin, synaptotagmin, synapsin I and annexin II (see Table S1), as reported previously in other proteomic studies of synaptosomes (Witzman et al., 2005). Prior screening studies of synaptosomes using isotope-coded affinity tags, however, have also shown some contamination by astrocytes (Schrimpf et al., 2005). Similarly, we found evidence of astrocytic markers, including GFAP and vimentin (Table 1). In fact, in line with the known astrogliosis that represents a neuropathological hallmark of HAND, we found that GFAP was quite significantly upregulated in HIV/gp120 transgenic mouse brain compared to control.

In order to determine the biochemical pathway(s) responsible for the differential proteomic profile in HIV/gp120 transgenic mice versus wt control littermates, we used bioinformatics pathway analysis tools. This analysis revealed that the pathway with the highest score, and thus most affected in HIV/gp120 transgenic brains, involved dysregulation in the PI3K/Akt cascade. We then confirmed these findings using immunoblot analysis on synaptosomes and forebrain lysates from HIV/gp120 transgenic mice as well as from human cortex from patients with and without HAND. As expected from samples from a heterogeneous population, the pAkt levels of autopsy brain showed minor variations within each group, which may also be affected by post-mortem intervals, other opportunistic infections in HIV+ cases or stage of HAND. These assays revealed a strong correlation between decreased Akt activity/phosphorylation and the development of HAND (Fig. 3C). Thus, these results suggest that activation of the PI3K/Akt pathway could be potentially neuroprotective in HAND.

Along these lines, we and our colleagues have previously demonstrated pAkt-mediated neuroprotection in both in vitro and in vivo models of HAND (Digicaylioglu et al. 2004a; Kang et al. 2010). In this context, we have shown that synergistic activation of the PI3K/Akt pathway by erythropoietin (EPO) and insulin-like growth factor I (IGF-I) activates a number of neuroprotective pathways, including phosphorylation of glycogen synthase kinase (GSK) 3β with consequent inhibition of tau protein hyperphosporylation, inhibition of forkhead transcription factor, and activation of inhibitory proteins of apoptosis (Digicaylioglu and Lipton, 2001; Digicaylioglu et al., 2004b; Kang et al., 2010). Additionally, pAkt can phosphorylate and thereby inactivate human caspase-9. Because caspase-9 is a major activator of effector caspase-3, this action of pAkt may also contribute to neuroprotection (Kermer et al., 2000; Nitta et al., 2004; Thorne et al., 2004).

Moreover, to show causality of these effects, recently in the HIV/gp120 transgenic mouse model, we demonstrated that activation of the PI3K/Akt pathway in the brain decreases tau hyperphosphorylation and affords neuroprotection (Kang et al., 2010). pAkt also activates the downstream transcription factor target, NF-κB (Borderies et al., 2004; Digicaylioglu and Lipton, 2001), an effect that has been implicated in chemokine CCL2 and fractalkine-mediated neuroprotection in HAND (Meucci et al., 2000; Yao et al., 2009).

Taken together with prior work, our current findings support the notion that downregulation of the Akt pathway may be involved in the pathogenesis of HAND and suggest that targeted activation of Akt might be neuroprotective in this disorder. Within the complex regulation of Akt activation, autophosphorylation appears to play a significant role (Li et al., 2006). Our finding that SNO-Akt is significantly elevated in HIV/gp120 mouse brains and human HAND brains represents a potential mechanism for the pathological decrease in Akt activity observed in our studies since this would result in a decrement in autophosphorylation.

In conclusion, we show that the HIV/gp120 mouse is a valid model for the discovery of pathophysiologically relevant pathways in HIV-related dementias. This work also

emphasizes the importance of proteomic techniques, such as TMT, which in combination with bioinformatics tools can enhance our understanding of complex signaling crosstalk in animal models of neurodegenerative disorders. Our use of these techniques has demonstrated that the web of Akt pathways are potentially important targets for development of therapies for HAND and perhaps other dementias.

Supplementary Material

Refer to Web version on PubMed Central for supplementary material.

Acknowledgments

This work was supported in part by NIH grants P01 HD29587, P01 ES016738, R01 NS047973, R01 EY09024, and Neuroscience Blueprint Core Grant P30 NS057096.

References

Borderies G, le Bechec M, Rossignol M, Lafitte C, Le Deunff E, Beckert M, Dumas C, Elisabeth MR. Characterization of proteins secreted during maize microspore culture: arabinogalactan proteins (AGPs) stimulate embryo development. Eur J Cell Biol. 2004; 83:205–212. [PubMed: 15346810]

Carlin RK, Grab DJ, Cohen RS, Siekevitz P. Isolation and characterization of postsynaptic densities from various brain regions: enrichment of different types of postsynaptic densities. J Cell Biol. 1980; 86:831–845. [PubMed: 7410481]

Che FY, Fricker LD. Quantitative peptidomics of mouse pituitary: comparison of different stable isotopic tags. J Mass Spectrom. 2005; 40:238–249. [PubMed: 15706629]

Cherner M, Masliah E, Ellis RJ, Marcotte TD, Moore DJ, Grant I, Heaton RK. Neurocognitive dysfunction predicts postmortem findings of HIV encephalitis. Neurology. 2002; 59:1563–1567. [PubMed: 12451198]

Cohen SA, Fischbach GD. Clusters of acetylcholine receptors located at identified nerve-muscle synapses in vitro. Dev Biol. 1977; 59:24–38. [PubMed: 892219]

Digicaylioglu M, Lipton SA. Erythropoietin-mediated neuroprotection involves cross-talk between Jak2 and NF-kappaB signalling cascades. Nature. 2001; 412:641–647. [PubMed: 11493922]

Digicaylioglu M, Kaul M, Fletcher L, Dowen R, Lipton SA. Erythropoietin protects cerebrocortical neurons from HIV-1/gp120-induced damage. Neuroreport. 2004a; 15:761–763. [PubMed: 15073510]

Digicaylioglu M, Garden G, Timberlake S, Fletcher L, Lipton SA. Acute neuroprotective synergy of erythropoietin and insulin-like growth factor I. Proc Natl Acad Sci U S A. 2004b; 101:9855–9860. [PubMed: 15210945]

Eng JM, McCormack AL, Yates JR III. An approach to correlate tandem mass spectral data of peptides with amino acid sequences in a protein database. J Am Soc Mass Spectrom. 1994; 5:976–989.

Garden GA, Budd SL, Tsai E, Hanson L, Kaul M, D'Emilia DM, Friedlander RM, Yuan J, Masliah E, Lipton SA. Caspase cascades in human immunodeficiency virus-associated neurodegeneration. J Neurosci. 2002; 22:4015–4024. [PubMed: 12019321]

Gorantla S, Liu J, Sneller H, Dou H, Holguin A, Smith L, Ikezu T, Volsky DJ, Poluektova L, Gendelman HE. Copolymer-1 induces adaptive immune anti-inflammatory glial and neuroprotective responses in a murine model of HIV-1 encephalitis. J Immunol. 2007; 179:4345–4356. [PubMed: 17878329]

Gygi SP, Rist B, Gerber SA, Turecek F, Gelb MH, Aebersold R. Quantitative analysis of complex protein mixtures using isotope-coded affinity tags. Nat Biotechnol. 1999; 17:994–999. [PubMed: 10504701]

Hansson E, Ronnback L. Glial neuronal signaling in the central nervous system. FASEB J. 2003; 17:341–348. [PubMed: 12631574]

Jaffrey SR, Erdjument-Bromage H, Ferris CD, Tempst P, Snyder SH. Protein S-nitrosylation: a physiological signal for neuronal nitric oxide. Nat Cell Biol. 2001; 3:193–197. [PubMed: 11175752]

Kang YJ, Digicaylioglu M, Russo R, Kaul M, Achim CL, Fletcher L, Masliah E, Lipton SA. Erythropoietin plus insulin-like growth factor-I protects against neuronal damage in a murine model of human immunodeficiency virus-associated neurocognitive disorders. Ann Neurol. 2010; 68:342–352. [PubMed: 20818790]

Kaul M, Ma Q, Medders KE, Desai MK, Lipton SA. HIV-1 coreceptors CCR5 and CXCR4 both mediate neuronal cell death but CCR5 paradoxically can also contribute to protection. Cell Death Differ. 2007; 14:296–305. [PubMed: 16841089]

Kennedy MB, Bennett MK, Erondu NE. Biochemical and immunochemical evidence that the “major postsynaptic density protein” is a subunit of a calmodulin-dependent protein kinase. Proc Natl Acad Sci U S A. 1983; 80:7357–7361. [PubMed: 6580651]

Kermer P, Klocker N, Labes M, Bahr M. Insulin-like growth factor-I protects axotomized rat retinal ganglion cells from secondary death via PI3-K-dependent Akt phosphorylation and inhibition of caspase-3 In vivo. J Neurosci. 2000; 20:2–8. [PubMed: 10632601]

Kolson DL. Neuropathogenesis of central nervous system HIV-1 infection. Clin Lab Med. 2002; 22:703–717. [PubMed: 12244593]

Li X, Lu Y, Jin W, Liang K, Mills GB, Fan Z. Autophosphorylation of Akt at Threonine 72 and Serine 246: A potential mechanism of regulation of Akt kinase activity. J Biol Chem. 2006; 281:13837–13843. [PubMed: 16549426]

McArthur JC. HIV dementia: an evolving disease. J Neuroimmunol. 2004; 157:3–10. [PubMed: 15579274]

McArthur JC, Steiner J, Sacktor N, Nath A. Human immunodeficiency virus-associated neurocognitive disorders: Mind the gap. Ann Neurol. 2010; 67:699–714. [PubMed: 20517932]

Meucci O, Fatatis A, Simen AA, Miller RJ. Expression of CX3CR1 chemokine receptors on neurons and their role in neuronal survival. Proc Natl Acad Sci U S A. 2000; 97:8075–8080. [PubMed: 10869418]

Moore DJ, Masliah E, Rippeth JD, Gonzalez R, Carey CL, Cherner M, Ellis RJ, Achim CL, Marcotte TD, Heaton RK, Grant I. Cortical and subcortical neurodegeneration is associated with HIV neurocognitive impairment. AIDS. 2006; 20:879–887. [PubMed: 16549972]

Numajiri N, Takasawa K, Nishiya T, Hayakawa W, Asada M, Matsuda H, Azumi K, Tanaka H, Hyakkoku K, Kamata H, Nakamura T, Hara H, Minami M, Lipton SA, Uehara T. On-off system for PI3-kinase-Akt signaling through S-nitrosylation of phosphatase with sequence homology to tensin (PTEN). Proc Natl Acad Sci USA. 2011; 108:10349–10354. [PubMed: 21646525]

Nitta A, Zheng WH, Quirion R. Insulin-like growth factor 1 prevents neuronal cell death induced by corticosterone through activation of the PI3k/Akt pathway. J Neurosci Res. 2004; 76:98–103. [PubMed: 15048933]

Park SK, Venable JD, Xu T, Yates JR III. A quantitative analysis software tool for mass spectrometry-based proteomics. Nat Methods. 2008; 5:319–322. [PubMed: 18345006]

Potula R, Poluektova L, Knipe B, Chrastil J, Heilman D, Dou H, Takikawa O, Munn DH, Gendelman HE, Persidsky Y. Inhibition of indoleamine 2,3-dioxygenase (IDO) enhances elimination of virus-infected macrophages in an animal model of HIV-1 encephalitis. Blood. 2005; 106:2382–2390. [PubMed: 15961516]

Ross A, Kessler W, Krumme D, Menge U, Wissing J, van den Heuvel J, Flohe L. Optimised fermentation strategy for 13C/15N recombinant protein labelling in Escherichia coli for NMR-structure analysis. J Biotechnol. 2004; 108:31–39. [PubMed: 14741767]

Schifitto G, Navia BA, Yiannoutsos CT, Marra CM, Chang L, Ernst T, Jarvik JG, Miller EN, Singer EJ, Ellis RJ, Kolson DL, Simpson D, Nath A, Berger J, Shriver SL, Millar LL, Colquhoun D, Lenkinski R, Gonzalez RG, Lipton SA. Memantine and HIV-associated cognitive impairment: a neuropsychological and proton magnetic resonance spectroscopy study. AIDS. 2007; 21:1877–1886. [PubMed: 17721095]

Schrimpf SP, Meskenaite V, Brunner E, Rutishauser D, Walther P, Eng J, Aebersold R, Sonderegger P. Proteomic analysis of synaptosomes using isotope-coded affinity tags and mass spectrometry. Proteomics. 2005; 5:2531–2541. [PubMed: 15984043]

Tabb DL, McDonald WH, Yates JR III. DTASelect and Contrast: tools for assembling and comparing protein identifications from shotgun proteomics. J Proteome Res. 2002; 1:21–26. [PubMed: 12643522]

Thorne RG, Pronk GJ, Padmanabhan V, Frey WH II. Delivery of insulin-like growth factor-I to the rat brain and spinal cord along olfactory and trigeminal pathways following intranasal administration. Neuroscience. 2004; 127:481–496. [PubMed: 15262337]

Toggas SM, Masliah E, Rockenstein EM, Rall GF, Abraham CR, Mucke L. Central nervous system damage produced by expression of the HIV-1 coat protein gp120 in transgenic mice. Nature. 1994; 367:188–193. [PubMed: 8114918]

Washburn MP, Wolters D, Yates JR III. Large-scale analysis of the yeast proteome by multidimensional protein identification technology. Nat Biotechnol. 2001; 19:242–247. [PubMed: 11231557]

Witzman FA, Arnold RJ, Bai F, Hrncirova P, Kimpel MW, Mechref YS, McBride WJ, Novotny MV, Pedrick NM, Ringham HN, Simon JR. A proteomic survey of rat cerebral cortical synaptosomes. Proteomics. 2005; 5:2177–2201. [PubMed: 15852343]

Yao H, Peng F, Dhillon N, Callen S, Bokhari S, Stehno-Bittel L, Ahmad SO, Wang JQ, Buch S. Involvement of TRPC channels in CCL2-mediated neuroprotection against tat toxicity. J Neurosci. 2009; 29:1657–1669. [PubMed: 19211873]

Yasukawa T, Tokunaga E, Ota H, Sugita H, Martyn JA, Kaneki M. S-Nitrosylation-dependent inactivation of Akt/protein kinase B in insulin resistance. J Biol Chem. 2005; 280:7511–7518. [PubMed: 15632167]

Abbreviations

HAND	HIV-associated neurocognitive disorders
TMT	tandem mass tag
MS/MS	tandem mass spectrometry
PQD	pulsed-Q dissociation
HAART	Highly-Active Antiretroviral Therapy
ICAT	Isotope Coded Affinity Tag
PSD95	postsynaptic density protein 95

Highlights

>Synaptosomes from HIV/gp12 Tg mice tandem mass tag labeled for MS/MS analysis. >Akt pathway identified as suppressed in HIV/gp12 Tg brains. > Akt pathway also suppressed in human HIV associated neurocognitive disorders (HAND). >Akt is S-nitrosylated in HIV/gp120 and HAND brain. >MS/MS and pathway analysis is means to identify potential drug targets in disease.

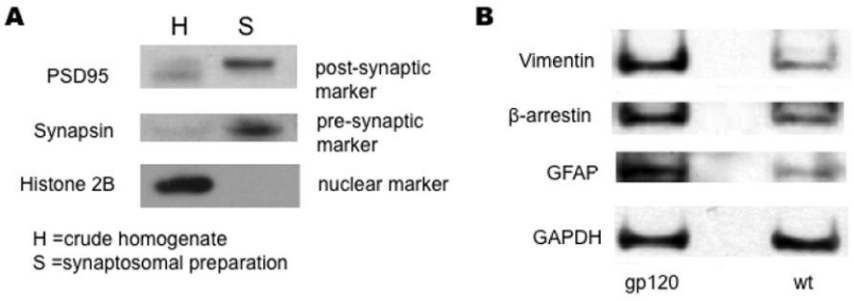

Figure 1.

Characterization of synaptosomal isolates from wt and HIV/gp120 transgenic mice. Immunoblot analysis of synaptosomal preparations from wt and HIV/gp120 transgenic mice. (A) Synaptosomal preparations (S) from wt and HIV/gp120 transgenic animals displayed greater expression of synapsin (a presynaptic marker) and PSD95 (a post-synaptic marker) than crude homogenates (H) from these animals. The crude homogenates manifested greater expression of the nuclear marker Histone H2B than the synaptosomal fraction. (B) Synaptosomes from HIV/gp120 transgenic mice displayed greater expression of vimentin, β-arrestin, and GFAP compared to wt littermate animals. In contrast, the glycolytic enzyme GAPDH was found at similar levels in both wt and transgenic animals.

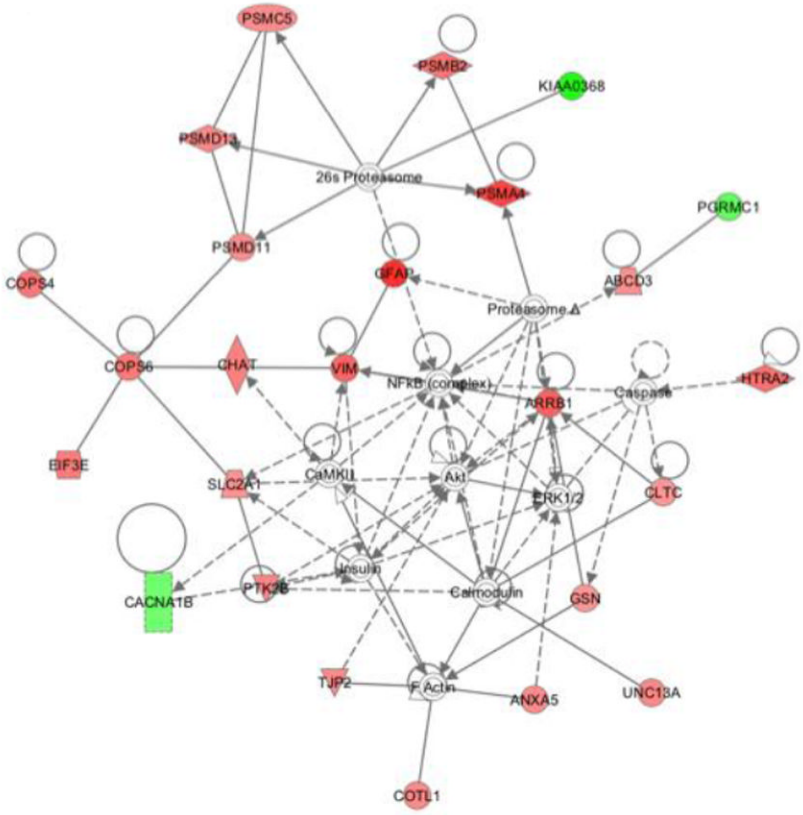

Figure 2.

Ingenuity pathway analysis of differentially regulated proteins. Pathway/network modeling of the synaptosomal proteome was determined by integration of our protein/gene data into Ingenuity Pathway Analysis software. Pathway analysis demonstrated direct or indirect involvement of the Akt cascade with the various differentially regulated proteins. Lines indicate known interactions (collected in Ingenuity Pathways Knowledge Base) among various proteins. The lines with arrowheads represent direct interactions. Solid lines with arrowheads show direct interaction, while broken arrowhead lines show indirect interaction. Lines without arrowheads indicate binding. Nodes are represented by shapes and colors. Protein function is indicated by shape: diamonds for enzymes, squares for cytokines, rectangles for ligand-dependant nuclear factors, triangles for kinases, ovals for transcriptional regulators, trapezoids for transporters, and circles for other types of actions. Red nodes represent the synaptosomal proteins we found to be upregulated in HIV/gp120 mouse brain, while the green nodes represent downregulated proteins. Nodes without color represent proteins not from our list, but interpreted by the database as highly probable interactions within the network. Abbreviations: ABCD3: ATP-binding cassette, sub-family D (ALD), member 3; ANXA5: annexin A5; ARRB1: arrestin, beta 1; CACNA1B: calcium channel, voltage-dependent, N type, alpha 1B; CaMKII: Calcium dependent protein kinase II; CHAT: choline acetyltransferase; CLTC: clathrin, heavy chain (Hc); COPS4: COP9 constitutive photomorphogenic homolog subunit 4; COPS6: COP9 constitutive photomorphogenic homolog subunit 6; COTL1: coactosin-like 1; EIF3E: (Dictyostelium) eukaryotic translation initiation factor 3 subunit E; GFAP: glial fibrillary acidic protein; GSN: gelsolin; HTRA2: HtrA serine peptidase 2; KIAA0368: Proteasome-associated protein ECM29 homolog; NFκB (complex): Nuclear factor κB; PGRMC1: progesterone receptor membrane component 1; PSMA4: proteasome subunit, alpha type, 4; PSMB2:proteasome

subunit, beta type; 2PSMC5:proteasome 26S subunit, ATPase; PSMD11:proteasome 26S subunit, non-ATPase 11; PSMD13: proteasome 26S subunit, non-ATPase, 13; PTK2B: PTK2B protein tyrosine kinase 2 β; SLC2A1: solute carrier family 2 (facilitated glucose transporter); TJP2: tight junction protein 2; UNC13A: unc-13 homolog A; VIM: vimentin.

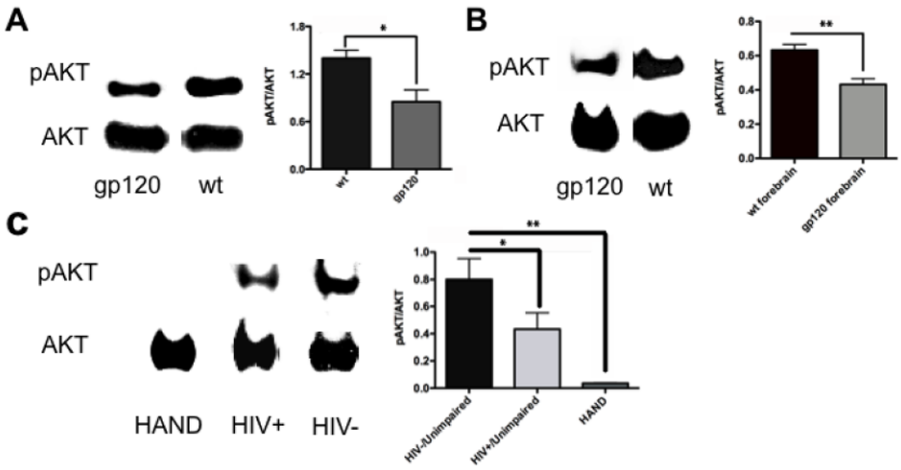

Figure 3.

Downregulation of pAkt levels in HIV/gp120 transgenic mice and human HIV-1 brains. Immunoblot and densitometric estimates of pAkt/Akt levels. (A) Synaptosomes of HIV/gp120 transgenic mice showed a significant decrease in pAkt/Akt levels compared to wt littermate animals. (B) Forebrain of HIV/gp120 transgenic mice also showed a significant reduction in pAkt/Akt levels compared to wt animals. (C) pAkt/total Akt ratio in frontal cortex of patients who were normal/HIV- (and unimpaired on neuropsychological testing), HIV+/unimpaired, and HIV+/HAND. Only the subjects with HAND showed a significant reduction in pAkt/Akt levels. Note that pAkt/Akt ratio tracked more closely with neuropsychological scores than with neuropathological assessments (Table 2). Values in histograms are mean + S.E.M. from $n \geq 3$ experiments (*$P < 0.05$, ** $P < 0.01$).

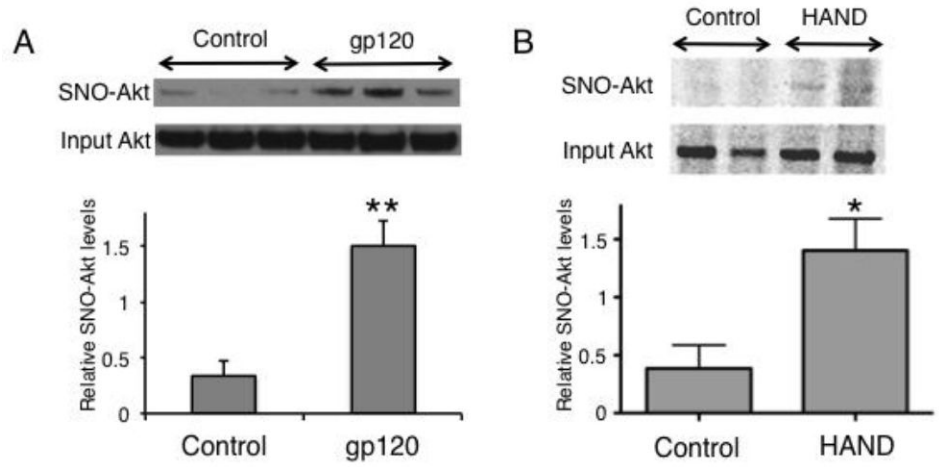

Figure 4.

S-nitrosylation of Akt is increased in HIV/gp120 mouse and human HAND brains. (A) HIV/gp120 mouse brain lysates were analyzed for S-nitrosylated (SNO)-Akt using the biotin-switch technique. Control lysates were from wt littermates ($n = 6$; $^{**}P < 0.01$ by t-test). (B) Lysates from human brain autopsy tissue of patients with HAND or non-neurological conditions (Controls) were analyzed by the biotin-switch technique for SNO-Akt ($n = 8$; $^{*}P < 0.02$ by t-test).

Table 1

Proteomic fingerprint of differentially regulated proteins (≥1.5 fold) in synaptosomal isolates from HIV/gp120 transgenic mice compared to wild-type animals*

ID	Symbol	Entrez Gene Name	Average Fold Change
Upregulated Proteins			
IPI00649033	GFAP	glial fibrillary acidic protein	3.2
IPI00351246	MPP3	membrane protein, palmitoylated 3	3.0
IPI00277001	PSMA4	proteasome (prosome, macropain) subunit, alpha type, 4	2.7
IPI00761566	ARRB1	arrestin, beta 1	2.3
IPI00227299	VIM	vimentin	2.2
IPI00474073	MAPRE2	microtubule-associated protein, RP/EB family, member 2	2.2
IPI00468204	AMPD3	adenosine monophosphate deaminase (isoform E)	2.1
IPI00131292	SLC22A4	solute carrier family 22 member 4	2.1
IPI00120798	SYT12	synaptotagmin XII	2.1
IPI00626662	ALDH1A1	aldehyde dehydrogenase 1 family, member A1	2.1
IPI00830249	HTRA2	HtrA serine peptidase 2	2.1
IPI00114801	INPP1	inositol polyphosphate-1-phosphatase	2.1
IPI00620701	RABGGTA	Rab geranylgeranyltransferase, alpha subunit	2.0
IPI00845733	PPM1H	protein phosphatase 1H (PP2C domain containing)	2.0
IPI00128945	PSMB2	proteasome subunit, beta type, 2	2.0
IPI00857710	COPS4	COP9 constitutive photomorphogenic homolog subunit 4	1.9
IPI00754071	PRDX6	peroxiredoxin 6	1.9
IPI00830393	COPS6	COP9 constitutive photomorphogenic homolog subunit 6	1.9
IPI00132250	EIF3E	eukaryotic translation initiation factor 3, subunit E	1.9
IPI00762185	MPST	mercaptopyruvate sulfurtransferase	1.9
IPI00224045	CHAT	choline acetyltransferase	1.8
IPI00894579	PGD	phosphogluconate dehydrogenase	1.8
IPI00331745	LXN	latexin	1.8
IPI00116138	HARS2	histidyl-tRNA synthetase 2, mitochondrial	1.8
IPI00857222	OXNAD1	oxidoreductase NAD-binding domain containing 1	1.8
IPI00608064	FECH	ferrochelatase (protoporphyria)	1.7
IPI00876210	CNIH3	cornichon homolog 3	1.7
IPI00310105	PTK2B	PTK2B protein tyrosine kinase 2 beta	1.7
IPI00132575	COTL1	coactosin-like 1 (Dictyostelium)	1.7
IPI00126048	PSMD13	proteasome 26S subunit, non-ATPase, 13	1.7
IPI00405121	UNC13A	unc-13 homolog A	1.7
IPI00225961	PHGDH	phosphoglycerate dehydrogenase	1.7
IPI00649885	ACADVL	acyl-Coenzyme A dehydrogenase, very long chain	1.7
IPI00323349	TJP2	tight junction protein 2 (zona occludens 2)	1.7
IPI00469268	CCT8	chaperonin containing TCP1, subunit 8 (theta)	1.7
IPI00317309	ANXA5	annexin A5	1.7
IPI00875497	CRAT	carnitine acetyltransferase	1.7

ID	Symbol	Entrez Gene Name	Average Fold Change
IPI00284521	DOCK3	dedicator of cytokinesis 3	1.7
IPI00112630	GLOD4	glyoxalase domain containing 4	1.6
IPI00460631	ICA1	islet cell autoantigen 1	1.6
IPI00454082	KIF21A	kinesin family member 21A	1.6
IPI00118821	PAFAH1B2	platelet-activating factor acetylhydrolase Ib, subunit 2	1.6
IPI00624863	PAICS	phosphoribosylaminoimidazole carboxylase,	1.6
IPI00222515	PSMD11	proteasome 26S subunit, non-ATPase, 11	1.6
IPI00649914	MCART1	mitochondrial carrier triple repeat 1	1.6
IPI00462789	PSMC5	proteasome 26S subunit, ATPase, 5	1.6
IPI00869359	CCDC132	coiled-coil domain containing 132	1.6
IPI00421218	TLN2	talin 2	1.6
IPI00223497	PDE1A	phosphodiesterase 1A, calmodulin-dependent	1.6
IPI00130225	SNX4	sorting nexin 4	1.6
IPI00553576	ABCD3	ATP-binding cassette, sub-family D (ALD), member 3	1.6
IPI00322312	ARHGDIA	Rho GDP dissociation inhibitor (GDI) alpha	1.6
IPI00845557	CTBP1	C-terminal binding protein 1	1.6
IPI00755161	OSBP	oxysterol binding protein	1.6
IPI00884508	SLC2A1	solute carrier family 2, member 1	1.6
IPI00648173	CLTC	clathrin, heavy chain (Hc)	1.5
IPI00759948	GSN	gelsolin (amyloidosis, Finnish type)	1.5
IPI00116112	DCTN2	dynactin 2 (p50)	1.5
IPI00751036	EXOC1	exocyst complex component 1	1.5
IPI00135345	NUDT2	nudix (nucleoside diphosphate linked moiety X)-type motif 2	1.5
IPI00379202	LOC1001	similar to kinase D-interacting substrate 220	1.5
IPI00330523	PCCA	propionyl Coenzyme A carboxylase, alpha polypeptide	1.5
IPI00889265	NCDN	neurochondrin	1.5
IPI00467223	NCKIPSD	NCK interacting protein with SH3 domain	1.5
IPI00169524	TRHDE	thyrotropin-releasing hormone degrading enzyme	1.5
IPI00341302	C8ORF38	chromosome 8 open reading frame 38	1.5
IPI00312752	SH3GL1	SH3-domain GRB2-like 1	1.5
IPI00756786	SH3GLB2	SH3-domain GRB2-like endophilin B2	1.5
IPI00131695	ALB	albumin	1.5
IPI00317711	HSPA4L	heat shock 70kDa protein 4-like	1.5
IPI00116277	CCT4	chaperonin containing TCP1, subunit 4 (delta)	1.5
IPI00331174	CCT7	chaperonin containing TCP1, subunit 7 (eta)	1.5
IPI00229893	MARK4	MAP/microtubule affinity-regulating kinase 4	1.5
IPI00314467	PSMB3	proteasome subunit, beta type, 3	1.5
IPI00114279	SLC1A3	solute carrier family 1 member 3	1.5
IPI00473685	USP14	ubiquitin specific peptidase 14 (tRNA-guanine transglycosylase)	1.5
Downregulated Proteins			
IPI00554917	CLCN6	chloride channel 6	-2.7
IPI00315794	CYB5B	cytochrome b5 type B	-2.5

ID	Symbol	Entrez Gene Name	Average Fold Change
IPI00553357	KIAA0368	KIAA0368	-2.5
IPI00649734	CROCC	rootletin	-2.4
IPI00117986	SLC12A9	solute carrier family 12 (K+/Cl- transporters)	-2.1
IPI00462406	PITPNM2	phosphatidylinositol transfer protein, membrane-associated 2	-2.1
IPI00338327	NDRG3	NDRG family member 3	-2.0
IPI00420535	ISLR2	immunoglobulin superfamily containing leucine-rich repeat 2	-1.9
IPI00337980	RAB21	RAB21, member RAS oncogene family	-1.9
IPI00121378	ALCAM	activated leukocyte cell adhesion molecule	-1.9
IPI00658743	APOO	apolipoprotein O	-1.8
IPI00319973	PGRMC1	progesterone receptor membrane component 1	-1.8
IPI00914696	ILDR2	immunoglobulin-like domain containing receptor 2	-1.7
IPI00133006	NDUFAB1	NADH dehydrogenase (ubiquinone) 1,	-1.7
IPI00652675	LSAMP	limbic system-associated membrane protein	-1.7
IPI00378120	GLRX5	glutaredoxin 5	-1.7
IPI00555118	SLC4A10	solute carrier family 4, sodium bicarbonate transporter	-1.7
IPI00356063	SCN2B	sodium channel, voltage-gated, type II, beta	-1.6
IPI00125787	GM14072	predicted gene 14072	-1.6
IPI00466672	CACNA1B	calcium channel, voltage-dependent, N type, alpha 1B	-1.6
IPI00653706	FAM126B	family with sequence similarity 126, member B	-1.5
IPI00461629	FXN	frataxin	-1.5
IPI00622742	CAPN2	calpain 2, (m/II) large subunit	-1.5
IPI00551399	EFR3A	EFR3 homolog A	-1.5
IPI00129298	PALM	paralemmin	-1.5
IPI00127447	SCARB2	scavenger receptor class B, member 2	-1.5
IPI00881362	ZFPL1	zinc finger protein-like 1	-1.5
IPI00323809	PALM	paralemmin	-1.5
IPI00461730	PGAM5	phosphoglycerate mutase family member 5	-1.5
IPI00331284	VTI1B	vesicle transport through interaction with t-SNAREs 1B	-1.5
IPI00331463	ATPIF1	ATPase inhibitory factor 1	-1.5

*A positive-fold change indicates an increase and a negative-fold change indicates a decrease in the indicated protein in HIV/gp120 mice.

Exp Neurol. Author manuscript; available in PMC 2013 August 01.

Table 2

Patient characteristics of cases evaluated for pAKT and SNO-Akt levels

Group	AGE	SEX	Post-mortem Interval	Neuropathology	GDS	Neuropsychology
Normal/(HIV-)	63	Female	8	Normal	N/A	Unknown
Normal//(HIV-)	69	Male	24	Normal	N/A	Unknown
Normal/(HIV-)	71	Male	2	Normal	N/A	Unknown
HIV+	51	Male	17	Normal	<0.5	Normal
HIV+	59	Female	15	HIV encephalitis	<0.5	Normal
HIV+	40	Male	13	Microglial nodule encephalitis	<0.5	Normal
HIV+	50	Male	15	Normal	0.67	MCMD
HIV+	55	Male	15	HIV encephalitis	2.37	HAD
HIV+	51	Male	48	HIV encephalitis, Leukoencephalopathy	2.94	HAD

HIV+: HIV-1 infected
HAD: HIV-associated dementia
MCMD: Minor cognitive and motor disorder
(HAD represents severe and MCMD represents mild forms of HAND)
GDS: Global Deficit score; >0.5 is a criterion for HAND
Brain region used: Frontal cortex